Turbulence transport within the Heliosphere

13th Annual International Astrophysics Conference: Voyager, IBEX, and the Interstellar Medium IOP Publishing
Journal of Physics: Conference Series **577** (2015) 012001 doi:10.1088/1742-6596/577/1/012001

Turbulence transport within the Heliosphere

L Adhikari[1,2], G P Zank[1,2], R Bruno[3], D Telloni[3], P Hunana[2], and A Dosch[2]

[1]Department of Space Science, University of Alabama in Huntsville, Huntsville, AL 35899, USA
[2]Center for Space Plasma and Aeronomic Research (CSPAR), University of Alabama in Huntsville, Huntsville,
AL 35899, USA
[3] AA(INAF-IAPS Istituto di Astrofisica e Planetologia Spaziali, Via del Fosso del Cavaliere 100, 00133 Roma, Italy

E-mail: la0004@uah.edu

Abstract. This work continues the investigation of turbulence transport throughout the supersonic solar wind initiated in Zank et al 1996 [27] and Zank et al 2012 [20]. [20] developed a system of six coupled transport equations that describe the transport of energy corresponding to forward propagating (g) and backward propagating modes (f), the residual energy (E_D), and the correlation lengths corresponding to forward propagating modes (λ^-), backward propagating modes (λ^+), and the correlation length (λ_D) for residual energy. These models can be applied to both sub-Alfvénic (such as the lower corona) and super-Alfvénic (e.g., supersonic solar wind and inner heliosheath) flows. The correlation lengths calculated from our model are in good agreement with those observed. The evolution of related parameters is also calculated from 0.29 AU to 5 AU.

1. Introduction

Turbulence is ubiquitous in space and astrophysical plasmas such as, the solar corona, the solar wind, accretion disks, the interstellar medium and so forth. The scattering of solar energetic particles ([1, 2]), the generation of the fast solar wind from open field regions of the solar corona ([3, 4, 5]), the observed non-adiabatic radial solar wind temperature profile ([6 - 12]), are all thought to be due to the effects of turbulence. The solar wind is an almost collisionless magnetized plasma, and is regarded as a huge laboratory for studying turbulence ([13, 14]). The theoretical and observational study of solar wind turbulence, despite intensive attention over the past decades, remains at the forefront of solar physics research. Here, we focus on one aspect, which is the evolution of fundamental turbulence quantities as a function of heliocentric distance.

Velocity and magnetic field fluctuations in the solar wind near the Sun are observed ([15, 16]) to be highly correlated, and satisfy the relation $\delta\mathbf{v} = \pm\delta\mathbf{B}/\sqrt{4\pi\rho}$, where $\delta\mathbf{v}$ and $\delta\mathbf{B}$ are velocity and magnetic field fluctuations, respectively and ρ is the solar wind density. These correlations are stronger at lower than higher frequencies. The sign in front of $\delta\mathbf{B}$ depends on $sign[-\mathbf{k}\cdot\mathbf{B}]$, where $\mathbf{k}$ and $\mathbf{B}$ are the wave vector and background magnetic field, respectively ($\delta\mathbf{v}$ and $\delta\mathbf{B}$ are parallel when the average interplanetary magnetic field is directed inwards with respect to the Sun and they are antiparallel when it is directed outwards). There exist both types of forward

and backward propagating modes below the Alfvén critical point (i.e., it is a point where the solar wind speed and Alfvén speed are equal); however the backward propagating modes in this region move faster than the solar wind speed, and hence always propagate towards the Sun. So, the only modes that escape from the sub-Alfvénic region are forward propagating modes. Thus, backward propagating modes beyond the Alfvén critical point are not of solar origin. Due to the presence of oppositely directed propagating modes, nonlinear interactions excite the cascade (i.e., the transfer of energy from larger scales to smaller scales) so that smaller scales energy eventually dissipate as heat energy. Usually the spectra of the fluctuations of the magnetic field in the solar wind exhibits a Kolmogorov-like scaling with a spectral slope of $-5/3$ in wavenumber space, and is due to the in situ generation of a turbulence cascade by dynamical processes ([14, 17]). An Iroshikov-Kraichnan-like scaling of $k^{-3/2}$, where k is the wave number ([18, 19]), is also observed sometimes in the solar wind.

The difference between the fluctuating kinetic and magnetic energies is known as the residual energy. The correlation between the square root of these two quantities is known as the cross helicity. The cross-helicity describes the equipartition of energy between forward and backward propagating modes. It decreases with increasing heliocentric distance, and is zero if the forward and backward propagating modes have the same energy. The heliocentric evolution of the energy in the forward and backward modes, and the corresponding residual energy and cross-helicity, is not particularly well understood observationally, and certainly not theoretically. Our purpose here is to solve the Zank et al 2012 [20] model that describes the transport of turbulence with heliocentric distance, and to compare the predicted correlation length with observations of the correlation length in the super-Alfvénic solar wind.

2. Background

The origin of the solar wind is the solar corona from where the solar wind expands supersonically into the heliosphere. The structure of the solar wind is very complex, and solar wind parameters, such as the solar wind velocity, the plasma density, the solar wind temperature, and the magnetic field fluctuate around their mean values. However, one can separate the mean field from the fluctuating fields, allowing us to express the magnetic and velocity fields as $\underline{\mathbf{B}} = \mathbf{B} + \mathbf{b}$ and $\underline{\mathbf{U}} = \mathbf{U} + \mathbf{u}$, where $\mathbf{B}$ and $\mathbf{U}$ are mean fields, and $\mathbf{b}$ and $\mathbf{u}$ are the fluctuating fields. Here, $\langle \underline{\mathbf{B}} \rangle = \mathbf{B}$, and $\langle \underline{\mathbf{U}} \rangle = \mathbf{U}$ meaning that the averaging procedure forces the rapidly varying fluctuating fields $\mathbf{b}$ and $\mathbf{u}$ to vanish. Furthermore, because of the solar cycle the time dependent mean fields fluctuate with time, and hence heliocentric distance [21].

The evolution and transport of fluctuations of velocity and magnetic fields can be described by the well-known two scale-separated incompressible MHD equations ([22 - 25]) in terms of the Elsässer variables as

$$\frac{\partial \mathbf{z}^{\pm}}{\partial t} + (\mathbf{U} \mp \mathbf{V}_A)\cdot\nabla \mathbf{z}^{\pm} + \frac{1}{2}\nabla\cdot(\mathbf{U}/2 \pm \mathbf{V}_A)\mathbf{z}^{\pm} + \mathbf{z}^{\mp}\cdot\left[\nabla \mathbf{U} \pm \frac{\nabla \mathbf{B}}{\sqrt{4\pi\rho}} - \frac{1}{2} I \nabla\cdot(\mathbf{U}/2 \pm \mathbf{V}_A)\right] = \mathbf{NL}_{\pm} + \mathbf{S}^{\pm}, \tag{1}$$

where I is the identity matrix, $\mathbf{NL}_{\pm}$ is a non-linear term that is responsible for the decay of turbulence, $\mathbf{S}^{\pm}$ is a source term, and $\mathbf{V_A}$ is the Alfvén velocity. Here, $\mathbf{z}^{\pm} = \mathbf{u} \pm \mathbf{b}/\sqrt{4\pi\rho}$ are the Elsässer variables ([26]), ρ is the solar wind density, and can be a function of both large-scales (e.g., solar wind scale) and small-scales (e.g., turbulence). Also, $\mathbf{z}^{+}$ ($\mathbf{z}^{-}$) represents the inward (outward) propagating modes with respect to the Sun.

By taking moments of equation (1) and imposing several assumptions (see [20] and [27]), Zank et al 1996 [27] developed a turbulent transport model that describes the transport and evolution of fluctuations of the fluctuating magnetic energy density (E_b) and correlation length (l) beyond 1-2 AU. However, [27] cannot describe the transport of turbulence within 1 AU since $\mathbf{V_A}$ was neglected and the cross helicity (E_c) was assumed to be zero, which is not observed to hold in the inner heliosphere ([28, 29]). The importance of [27] is that it reconciled the accepted turbulence

description of fluctuations in the solar wind with the observed WKB-like (i.e., a linear wave description) decay of magnetic energy within a fully turbulence-based transport model. Zank et al 1996 [27] found good agreement with observations from ~ 1 AU to 40 AU. Later [7], and [8] used the formalism of [27] to show that the observed radial solar wind temperature profile could be explained by the dissipation of the fluctuating magnetic energy density.

Breech et al 2008 [12] used an approach similar to that initiated by Zank et al 1996 [27] to include cross-helicity in a turbulence transport model. The model compared well with observations from 0.3 AU to 100 AU. However, Breech et al 2008 [12] cannot address the transport of turbulence in complex sub-Alfvénic flows nor do they include the residual energy. To address these problems, Zank et al 2012 [20] developed a system of six coupled turbulence transport equations by taking moments of equation (1), and developing a closure that allows application to both sub-Alfvénic and super-Alfvénic flows. The six coupled turbulence transport equations of [20] in terms of $f =< z^{+2} >$ and $g =< z^{-2} >$ with $a = 1/2$ and $b = 0$, are

$$\frac{\partial f}{\partial t} + (\mathbf{U} - \mathbf{V}_A)\cdot\nabla f + \frac{1}{2}\nabla\cdot\mathbf{U}f + \nabla\cdot\mathbf{V}_A f + \frac{1}{2}\nabla\cdot\mathbf{U}E_D - \Gamma E_D - \nabla\cdot\mathbf{V}_A E_D = -2\frac{fg^{1/2}}{\lambda} + 2\left\langle \mathbf{S}^+\cdot\mathbf{z}^+\right\rangle; \tag{2}$$

$$\frac{\partial g}{\partial t} + (\mathbf{U} + \mathbf{V}_A)\cdot\nabla g + \frac{1}{2}\nabla\cdot\mathbf{U}g - \nabla\cdot\mathbf{V}_A g + \frac{1}{2}\nabla\cdot\mathbf{U}E_D - \Gamma E_D + \nabla\cdot\mathbf{V}_A E_D = -2\frac{gf^{1/2}}{\lambda} + 2\left\langle \mathbf{S}^-\cdot\mathbf{z}^-\right\rangle; \tag{3}$$

$$\frac{\partial E_D}{\partial t} + \mathbf{U}\cdot\nabla E_D + \frac{1}{2}\nabla\cdot\mathbf{U}E_D + \frac{1}{2\sqrt{fg}}\left[f\mathbf{V}_A\cdot\nabla g - g\mathbf{V}_A\cdot\nabla f\right] + \left[\frac{1}{2}\nabla\cdot\mathbf{U} - \Gamma\right]\frac{f+g}{2} + \nabla\cdot\mathbf{V}_A\frac{f-g}{2} = -E_D\left[\frac{f^{1/2}}{\lambda^-} + \frac{g^{1/2}}{\lambda^+}\right] + \left\langle \mathbf{S}^-\cdot\mathbf{z}^+\right\rangle + \left\langle \mathbf{S}^+\cdot\mathbf{z}^-\right\rangle; \tag{4}$$

$$\frac{\partial\lambda^+}{\partial t} + (\mathbf{U} - \mathbf{V}_A)\cdot\nabla\lambda^+ + \frac{E_D}{f}\left[\frac{1}{4}\nabla\cdot\mathbf{U} - \frac{1}{2}\nabla\cdot\mathbf{V}_A - \frac{\Gamma}{2}\right]\left[\lambda_D - \lambda^+\right] = 2g^{1/2} - 2\frac{\left\langle \mathbf{z}^+\cdot\mathbf{S}^+\right\rangle}{f}\lambda^+; \tag{5}$$

$$\frac{\partial\lambda^-}{\partial t} + (\mathbf{U} + \mathbf{V}_A)\cdot\nabla\lambda^- + \frac{E_D}{g}\left[\frac{1}{4}\nabla\cdot\mathbf{U} + \frac{1}{2}\nabla\cdot\mathbf{V}_A - \frac{\Gamma}{2}\right]\left[\lambda_D - \lambda^-\right] = 2f^{1/2} - 2\frac{\left\langle \mathbf{z}^-\cdot\mathbf{S}^-\right\rangle}{g}\lambda^-; \tag{6}$$

$$\frac{\partial\lambda_D}{\partial t} + \mathbf{U}\cdot\nabla\lambda_D + 2\left(\frac{1}{4}\nabla\cdot\mathbf{U} - \frac{\Gamma}{2}\right)\frac{f+g}{E_D}\left(\frac{f\lambda^+ + g\lambda^-}{f+g} - \frac{\lambda_D}{2}\right) + \nabla\cdot\mathbf{V}_A\left(\frac{f\lambda^+ - g\lambda^-}{f-g} - \frac{\lambda_D}{2}\right)\frac{f-g}{E_D} + \frac{1}{2E_D\sqrt{fg}}\left(f\mathbf{V}_A\cdot\nabla g - g\mathbf{V}_A\cdot\nabla f\right)\left[2\left(\lambda^+\lambda^-\right)^{1/2} - \lambda_D\right] + \frac{\sqrt{fg}}{E_D}\left[\left(\frac{\lambda^+}{\lambda^-}\right)^{1/2}\mathbf{V}_A\cdot\nabla\lambda^- - \left(\frac{\lambda^-}{\lambda^+}\right)^{1/2}\mathbf{V}_A\cdot\nabla\lambda^+\right] = \lambda_D\left[\frac{f^{1/2}}{\lambda^-} + \frac{g^{1/2}}{\lambda^+}\right] - \frac{\lambda_D}{E_D}\left[\left\langle \mathbf{z}^-\cdot\mathbf{S}^+\right\rangle + \left\langle \mathbf{z}^+\cdot\mathbf{S}^-\right\rangle\right], \tag{7}$$

where f is the energy corresponding to backward propagating modes, g is the energy corresponding to forward propagating modes, $E_D = \left\langle u^2\right\rangle - \left\langle b^2/4\pi\rho\right\rangle$ is the residual energy, λ^+ is the correlation length corresponding to backward propagating modes, λ^- the correlation length corresponding to forward propagating modes, and λ_D is the correlation length corresponding to the residual energy. Terms such as $\left\langle \mathbf{S}^\pm\cdot\mathbf{z}^\pm\right\rangle$ refer to sources of turbulence, and can be due to the stream-shear interaction between fast and slow wind shock waves, and pick up ions. The parameter $\Gamma(= n_i n_j\frac{\partial U_j}{\partial U_i})$ is the shear mixing term, which we neglect by choosing $\Gamma = 0$.

An important implication of these models is that backward propagating modes can be generated due to the reflection of forward propagating modes. In the absence of Alfvén velocity, mixing, dissipation and source terms, equations (2), (3), and (4) reduce to the well-known WKB Model (see Appendix A).

3. Sources of Turbulence

There are in principle three types of turbulence sources, and which source is important depends on location in the heliosphere. Firstly, stream shear is an important source of turbulence ([15, 30]). Secondly, shock waves can generate turbulence as they propagate through the solar wind ([31]). Finally, pickup ions created by charge exchange between the solar wind protons and interstellar neutral hydrogen is an important source of turbulence ([27, 32]). The first two sources are important within 4 - 5 AU, and the last source is important beyond the ionization cavity ($\gtrsim$ 6 - 10 AU) ([10, 11, 27, 32]). Here, we consider the region from 0.29 AU to 5 AU, and so only the stream-shear source of turbulence is necessary to include.

The source term to model turbulence generated by shear interactions can be written in a form similar to that introduced in ([27]),

$$\left\langle \mathbf{S}^{+} \cdot \mathbf{z}^{+} \right\rangle = C_{sh}(f)\frac{\Delta U_{shear}}{r} f; \tag{8}$$

$$\left\langle \mathbf{S}^{-} \cdot \mathbf{z}^{-} \right\rangle = C_{sh}(g)\frac{\Delta U_{shear}}{r} g; \tag{9}$$

$$\left\langle \mathbf{S}^{-} \cdot \mathbf{z}^{+} \right\rangle + \left\langle \mathbf{S}^{+} \cdot \mathbf{z}^{-} \right\rangle = [C_{sh}(f) + C_{sh}(g)]\frac{\Delta U_{shear}}{r} E_D, \tag{10}$$

where $C_{sh}(f)$ and $C_{sh}(g)$ are the strengths of shear interaction for the backward and forward propagating modes, respectively, and ΔU_{shear} (= 350 km/s) is characteristic difference between the fast and slow solar wind speeds. Equations (8), (9), and (10) describe the shear source of turbulence for the backward, forward, and residual energy, respectively. Shear driving generally supplies equal energy to forward and backward types of fluctuations ([29]) [i.e., $C_{sh}(f) \sim C_{sh}(g)$]. The derivation of equation (10) is shown in Appendix B. Similarly, the source terms due to the presence of shocks, following the approach of ([27]), are

$$\left\langle \mathbf{S}^{+} \cdot \mathbf{z}^{+} \right\rangle = C_{shock}(f)\frac{\Delta U_{shock}}{r} f; \tag{11}$$

$$\left\langle \mathbf{S}^{-} \cdot \mathbf{z}^{-} \right\rangle = C_{shock}(g)\frac{\Delta U_{shock}}{r} g; \tag{12}$$

$$\left\langle \mathbf{S}^{-} \cdot \mathbf{z}^{+} \right\rangle + \left\langle \mathbf{S}^{+} \cdot \mathbf{z}^{-} \right\rangle = [C_{shock}(f) + C_{shock}(g)]\frac{\Delta U_{shock}}{r} E_D, \tag{13}$$

where $C_{shock}(f)$ and $C_{shock}(g)$ parametrize the generation of energy for the backward and forward propagating modes, respectively, and ΔU_{shock} is the difference between the upstream and downstream speed of the shock.

4. Method

The steady state 1D coupled system of equations [(2)-(7)] is solved in spherical coordinates, neglecting the θ and ϕ components. We used a Runge-Kutta 45 method. The solar wind was assumed to be spherically symmetric i.e., $\mathbf{U} = U_0\hat{r}$, where U_0 = 400 km/s is the solar wind

speed. The Alfvén velocity associated with the interplanetary magnetic field (Parker's model) is given by

$$V_A = \frac{B}{\sqrt{4\pi\rho}} = V_{A0}\left(\frac{R_0}{r}\right)\left[1+\left(\frac{\omega_0 R_0}{U_0}\right)^2\left(\frac{r}{R_0}-1\right)^2\sin^2\theta\right]^{1/2}, \tag{14}$$

where $R_0 = 10R_\odot$ ($R_\odot = 6.955\times10^5$ km is a solar radius), $V_{A0} = 400$ km/s is the Alfvén speed, $\omega_0 = 2.9\times10^{-6}$ rad/s is an angular speed of the Sun, and θ is colatitude with respect to solar rotation. We chose $\theta = \pi/2$ i.e., the ecliptic plane. The suffix 0 represents a reference point. The total turbulent energy E_T and the cross-helicity E_C can be calculated by using the following relations [20],

$$E_T = \frac{f+g}{2} = \langle\, u^2 \,\rangle + \langle\, b^2/4\pi\rho \,\rangle\,; \tag{15}$$

$$E_C = \frac{g-f}{2} = 2\left\langle\, \mathbf{u}\cdot\mathbf{b}/\sqrt{4\pi\rho}\,\right\rangle, \tag{16}$$

The inner boundary conditions for the turbulence variables at 0.29 AU are $f_0 = 753$ (km/s)^2, $g_0 = 13,515$ (km/s)^2, $E_{D0} = -57.07$ (km/s)^2, $\lambda_0^+ = 0.00143$ AU, $\lambda_0^- = 0.000779$ AU and $\lambda_{D0} = 0.00286$ AU. Also, we used $C_{sh}(f) \sim C_{sh}(g) = 16.35$. The suffix 0 represents a reference point which in our case is 0.29 AU.

5. Discussion

Here, we present solutions to the steady-state equations (2)-(7) for an expanding spherically symmetric flow in the presence of stream-shear driving. Theoretical results are shown in Figure 1 and a comparison of theoretically computed correlation lengths with observations from 0.29 AU to 5 AU is shown in Figure 2.

Figure (1) shows the numerical solution of our model [(2)-(7)] from 0.29 AU to 5 AU. The first column from top to bottom shows the total turbulent energy E_T, the energy corresponding to backward propagating modes f, and the correlation lengths (the dashed curve identifies λ^+, the dashed-dotted-dashed curve $\lambda_D/2$, and the solid curve λ^-), respectively. Similarly, the second column from top to bottom shows the energy corresponding to forward propagating modes g, the normalized residual energy $\bar{E}_D$ ($= E_D/E_T$), and the normalized cross-helicity $\bar{E}_C$ ($= E_C/E_T$), respectively. Fig.1 shows that the total energy in fluctuations $E_T = (< z^{+^2} > + < z^{-^2} >)/2$ decays uniformly from 0.29 AU to 5 AU despite the stream-shear source of turbulence. In our simple model of the stream-shear source, we have assumed that the source itself weakens with increasing heliocentric distance. Consequently, dissipation of $< z^{+^2} >$, $< z^{-^2} >$, and E_D ensure the overall decay of E_T. Note that we had introduced source terms into the WKB model, E_T would increase monotonically. Notice that g also decays monotonically, but f does not. An initial decrease in f is followed by an increase and then plateau followed by a slow decay with increasing heliocentric distance. The increase in f is due simply to the generation of backward propagating modes. The residual energy decays monotonically with radial distance reaching an approximately constant negative value beyond ~ 2.5 AU, showing that fluctuations in outer heliosphere are magnetically dominated. The cross-helicity also decays from a value of ~ 1 at 0.29 AU to 0.5 at 5 AU, reflecting the increase in f. Finally, all three of the correlation lengths $\lambda^\pm$, and λ_D increase with increasing heliocentric distance, despite the driving by shear. That the correlation lengths do not decrease reflects the weakening of the turbulence driving i.e., the dissipation proceeds more rapidly than the injection of energy.

Figure (2) is a comparison of the computed correlation lengths and those observed from 0.29 AU to 5 AU. The scattered "△"and "+"diagram show the observational correlation lengths for the backward and forward propagating modes, respectively. The dotted curve shows the correlation length corresponding to backward propagating modes, the solid curve

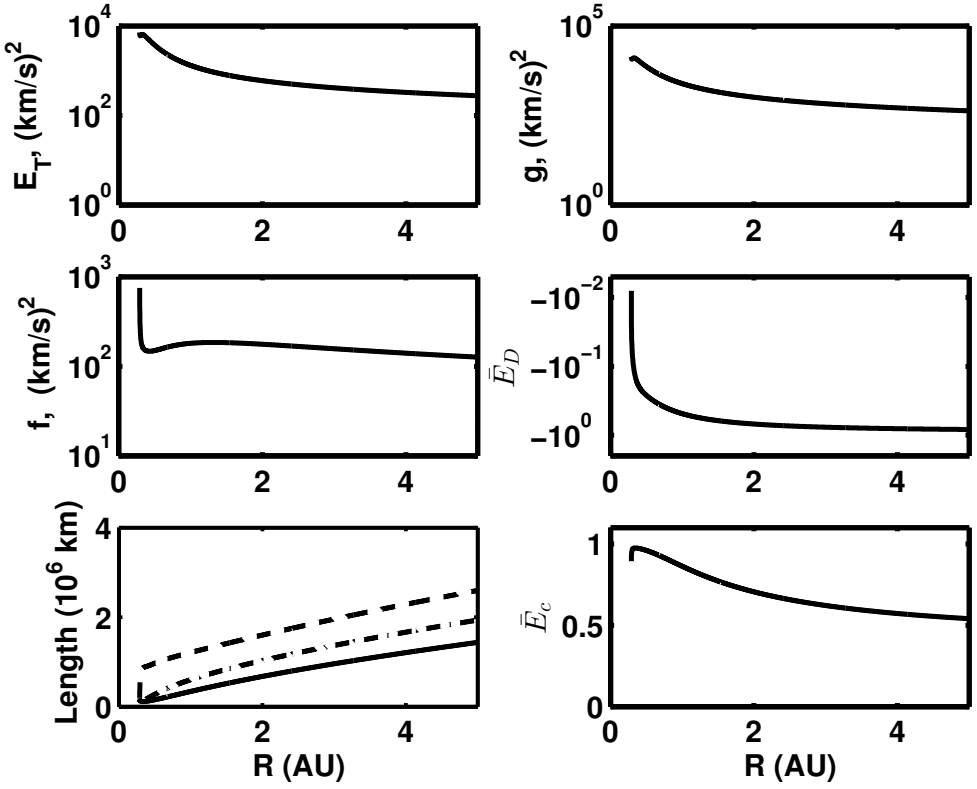

Figure 1. Solutions of the coupled turbulent transport equations [(2)-(7)] from 0.29 AU to 5 AU with turbulence driven by stream-shear. See text for details.

the correlation length corresponding to forward propagating modes, and the dashed-dotted-dashed curve denotes the (correlation length)/2 corresponding to the residual energy. Figures 3 and 4 correspond to Figures 1 and 2 except that shear driving has now has been neglected. The same format has been adopted.

The differences between Fig. 1 and Fig. 3 are apparent. All solutions decay but, in the absence of driving, the decay is more rapid. Two primary differences between the driven and undriven cases exist in the behavior of f and the correlation lengths. Without shear driving, although backward modes are generated, their energy nonetheless decays monotonically, unlike the driving case. In both cases, the correlation length increases with increasing heliocentric distance, but the scale is much larger for the undriven case. In the absence of driving, the dissipation rate does not have to increase as it does when driving present (this because the dissipation rate has to increase to balance the rate of energy injections.) Finally, the behavior of the residual energy and cross-helicity, while different in detail, like the driven case, decays with increasing heliocentric distance. As before, fluctuations become increasingly magnetic in character with distance from the Sun and the ratio between the energy in inward and outward propagating modes slowly tends to equalization.

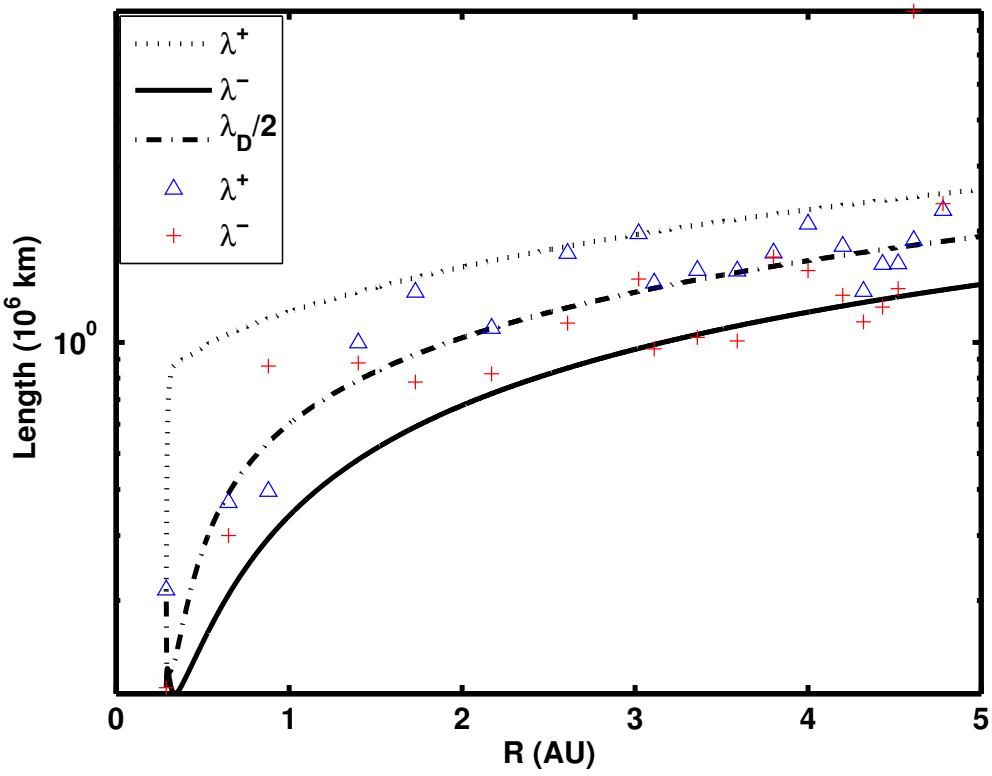

Figure 2. Comparison of the computed correlation lengths with those observed from 0.29 AU to 5 AU, assuming driving by stream-shear.

6. Conclusion

The turbulence transport models solved in this paper are more complex than previous models ([12, 27]), and they contain more information. The dependence on heliocentric distance for virtually all (non-spectral) quantities of interest to turbulence studies can be predicted on the basis of the Zank et al 2012 [20] model. We present the first numerical solution of this model, applicable to the region from 0.29 AU $\sim$ 5 AU. Furthermore, this model can be used to investigate turbulence in both sub-Aflvénic and super-Alfvénic flows. It is of course critical to validate complex models against observations. We make a start by comparing our computed correlation length with those observed between 0.29 AU and 5 AU. We find that the correlation lengths λ^+, λ^-, and $\lambda_D/2$ have some variation, but they show good agreement with the observation of the correlation length from 0.29 AU to 5 AU.

Acknowledgments

We acknowledge the partial support of NASA grants NNX14AC08G and NNX11AO64G.

Appendix A

Neglecting the Alfvén velocity, mixing, dissipation, and source terms, equations (2), (3), and (4) can be written as

$$\frac{\partial f}{\partial t} + \mathbf{U}\cdot\nabla f + \frac{1}{2}\nabla\cdot\mathbf{U}f = 0; \tag{17}$$

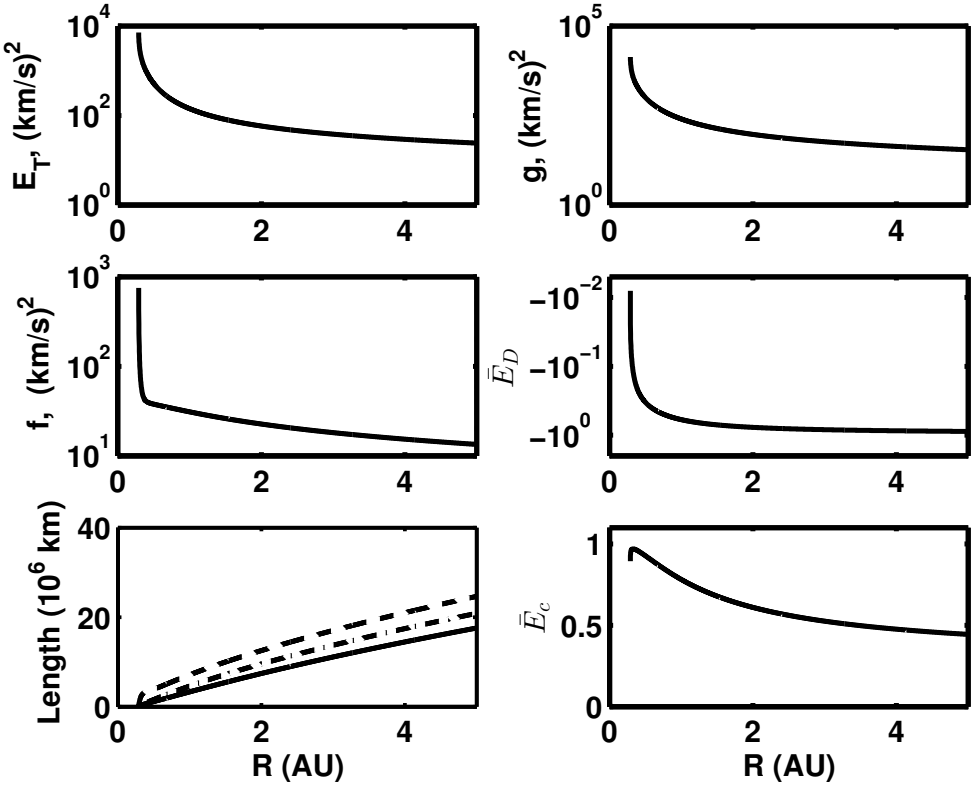

Figure 3. Solutions of the coupled turbulent transport equations [(2)-(7)] from 0.29 AU to 5 AU (without a source term).

$$\frac{\partial g}{\partial t} + \mathbf{U} \cdot \nabla g + \frac{1}{2} \nabla \cdot \mathbf{U} g = 0; \tag{18}$$

$$\frac{\partial E_D}{\partial t} + \mathbf{U} \cdot \nabla E_D + \frac{1}{2} \nabla \cdot \mathbf{U} E_D = 0. \tag{19}$$

Multiplying equation (19) by 2 and subtracting it from equations (17) and (18), we get

$$\frac{\partial \left(f + g - 2E_D \right)}{\partial t} + \mathbf{U} \cdot \nabla \left(f + g - 2E_D \right) + \frac{1}{2} \nabla \cdot \mathbf{U} \left(f + g - 2E_D \right) = 0, \tag{20}$$

which can be written in terms of the fluctuating magnetic energy density $E_b = (f + g - 2E_D)/4$ as

$$\frac{\partial E_b}{\partial t} + U \cdot \nabla E_b + \frac{1}{2} \nabla \cdot U E_b = 0, \tag{21}$$

Equation (21) is the well-known WKB model.

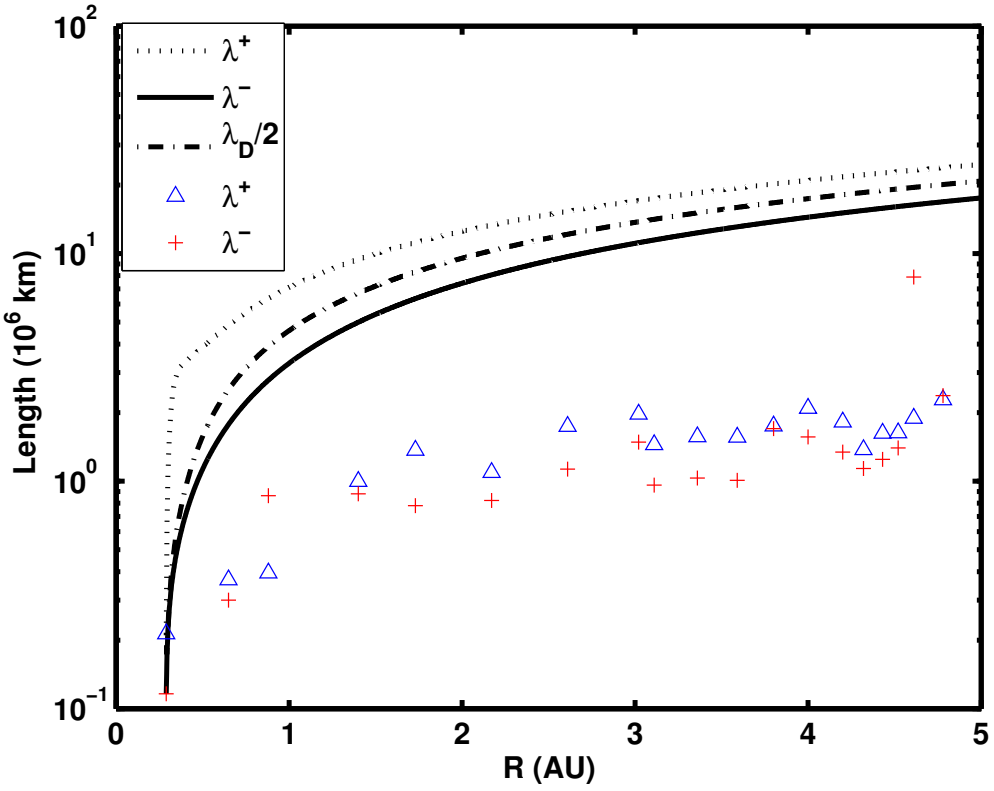

Figure 4. Comparison of the computed correlation lengths with those observed from 0.29 AU to 5 AU (without a source term).

Appendix B

The derivation of the source term for stream-shear interaction is straight forward,

$$\begin{aligned}\left\langle \mathbf{S}^{-}\cdot\mathbf{z}^{+}\right\rangle+\left\langle \mathbf{S}^{+}\cdot\mathbf{z}^{-}\right\rangle &= \left\langle C_{sh}(g)\frac{\Delta U}{r}\mathbf{z}^{-}\cdot\mathbf{z}^{+}\right\rangle+\left\langle C_{sh}(f)\frac{\Delta U}{r}\mathbf{z}^{+}\cdot\mathbf{z}^{-}\right\rangle \\ &= C_{sh}(g)\frac{\Delta U}{r}\left\langle \mathbf{z}^{-}\cdot\mathbf{z}^{+}\right\rangle+C_{sh}(f)\frac{\Delta U}{r}\left\langle \mathbf{z}^{+}\cdot\mathbf{z}^{-}\right\rangle \\ &= \left[C_{sh}(g)+C_{sh}(f)\right]\frac{\Delta U}{r}E_{D}\end{aligned}$$

7. References

[1] Li G, Zank G P, & Rice W K M 2003 *J. Geophys. Res. (Space Physics)* **108** 1082
[2] Zank G P, Li G & Verkhoglyadova O 2007 *Space Sci. Rev.* **130** 255
[3] Leer E, Holzer T E & Fla T 1982 *Space Sci. Rev.* **92** 11041
[4] Oughton S, Matthaeus W H, Dmitruk P 2001 *ApJ* **551** 565
[5] Verdini A, Velli M, Matthaeus W H, Oughton S & Dmitruk P 2010 *ApJ* **708** L116
[6] Williams L L, Zank G P, & Matthaeus W H 1995 *J. Geophys. Res.* **100** 17059
[7] Matthaeus W H, Zank G P, Smith C W and Oughton S 1999 Phys. Rev. Lett. **82** 3444
[8] Smith C W, Matthaeus W H, Zank G P 2001 *J. Geophys. Res.* **106** 8253
[9] Smith C W, Isenberg P A, Matthaeus W H, & Richardson J D 2006 *ApJ* **638** 508
[10] Isenberg P A, Smith C W, and Matthaeus W H 2003 *ApJ* **592** 564
[11] Isenberg P A 2005 *ApJ* **623** 502
[12] Breech B, Matthaeus W H, Minnie J 2008 *J. Geophys. Res.* **113** 8105

[13] Bavassano B, Dobrowolny M, Mariani F & Gosling N F 1982 *J. Geophys. Res.* **87** 3617
[14] Bruno R & Carbone V 2013 *Living Rev. in Solar Phys.* **10** 2
[15] Coleman Jr P J 1968 *ApJ* **153** 371
[16] Belcher J W & Davis Jr L 1971 *J. Geophys. Res.* **76** 3534
[17] Matthaeus W H & Goldstein M L 1982 *J. Geophys. Res.* **87** 6011
[18] Iroshnikov P S 1964 *Soviet Ast.* **7** 566
[19] Podesta J J, Roberts D A & Goldstein M L 2007 *ApJ* **664** 543
[20] Zank G P, Dosch A, Hunana P 2012 *ApJ* **745** 35
[21] Adhikari L, Zank G P, Hu Q, & Dosch A 2014 (Submitted to *ApJ*)
[22] Zhou Y & Matthaeus W H 1990 *J. Geophys. Res.* **95** 10291
[23] Zhou Y & Matthaeus W H 1990 *J. Geophys. Res.* **95** 14863
[24] Marsch T & Tu C 1989 *J. Geophys. Res.* **95** 8211
[25] Marsch T & Tu C 1989 *J. Geophys. Res.* **95** 11945
[26] Elsässer W M 1950 *Phys. Rev.* **79** 183
[27] Zank G P, Matthaeus W H and Smith C W 1996 *J. Geophys. Res.* **101** A8 17093-17107
[28] Matthaeus W H, Minnie J, Breech B 2004 *Geophys. Res. Lett.* **31** 12803
[29] Breech B, Matthaeus W H, Minnie J 2005 *Geophys. Res. Lett.* **32** 6103
[30] Roberts D A, Goldstein M L, Matthaeus W H, & Ghosh S 1992 *J. Geophys. Res.* **97** 17115
[31] Whang Y C 1991 *Space Sci. Rev.* **57** 339
[32] Williams L L & Zank G P 1994 *J. Geophys. Res.* **99** 19229